Contribution from the Departments of Chemistry, University of Iowa, Iowa City, Iowa 52242, and University of Notre Dame, Notre Dame, Indiana 46556

Synthesis, Molecular Structure, and Solution Properties of a Phenolate-Bridged (Tetraarylporphinato)iron(III) Dimer

HAROLD M. GOFF,*[1] ERIC T. SHIMOMURA,[1] YOUNG JA LEE,[2] and W. ROBERT SCHEIDT*[2]

Received June 1, 1983

The functionalized 5-(2-hydroxyphenyl)-10,15,20-tritolylporphyrin is prepared by mixed-aldehyde condensation, and iron is incorporated by standard procedures. Under basic hydrolytic conditions, intermolecular ligation of phenoxides to iron(III) centers is observed. A μ-oxo dimeric product is not detected under these conditions. The molecular structure of the phenolate dimer $((TTOP)Fe)_2$ was confirmed by X-ray crystallography. The toluene solvate crystallizes in a two-molecule orthorhombic cell with space group *P2na* and lattice constants a = 16.199 (2) Å, b = 14.408 (2) Å, and c = 18.622 (3) Å. A total of 4457 reflections were utilized to refine the structure. At convergence, R_1 = 0.049 and R_2 = 0.051. Porphyrin structural parameters are within ranges observed for other high-spin iron(III) complexes. The iron–oxygen distance of 1.847 (2) Å is comparable to that observed for non-porphyrin iron(III) phenolate complexes. Proton NMR spectra reveal pyrrole signals in the 80 ppm region diagnostic of a high-spin iron(III) center. Signals for the coordinated phenoxide groups are also observed in far-downfield and far-upfield regions. Reduction to the iron(II) state brings cleavage of phenoxide bridges, and proton NMR spectra are consistent with formation of a square-planar S = 1 (porphinato)iron(II) monomer. Air oxidation of this species in water-saturated toluene serves to regenerate the dimeric phenolate complex. The dimeric $((TTOP)Fe)_2$ exhibits solution and solid-state magnetic moments that match the spin-only value for high-spin iron(III). Antiferromagnetic coupling between metal centers is thus very small. No EPR spectrum was observed at 77 K as a consequence of efficient spin–spin electronic relaxation between metal centers separated by only 6.2 Å. Electrochemical measurements reveal two reversible reduction waves and complex overlapping oxidation waves. The dimeric phenolate complex has properties appropriate for a multielectron-redox catalyst.

Introduction

Metalloporphyrins are known to exhibit a variety of dimeric structures in which a ligand bridges two metal centers. Well-defined (porphinato)iron dimers are formed in which oxo,[3] nitrido,[4] carbido,[5] sulfato,[6] peroxo,[7] imidazolato,[8] pyrazine,[9] or hydroquinone[10] residues serve as bridges. Several covalently linked dimeric metalloporphyrins have also been reported in which a direct metal–ligand–metal bridge is not necessarily present.[11] Motivation for synthesis and physical study of dimeric species is found in the desire to (1) model multiple redox centers in enzymes such as cytochrome oxidase, (2) generate catalytic dioxygen reduction systems for use in fuel cells, and (3) gain a better understanding of electron transfer and spin–spin interactions between metal centers as a function of distance and bridging ligand.

The structure and solution properties of a novel dimeric phenolate (porphinato)iron(III) compound are reported here. Phenolate (porphinato)iron(III) complexes merit further attention on the basis of tyrosine coordination to (porphinato)iron(III) centers in catalase[12] and certain mutant hemoglobins.[13,14] Previous studies have addressed coordination, spectroscopic, and magnetic properties of phenolate (protoporphinato)iron(III) complexes,[14-16] and to a lesser extent the (tetraphenylporphinato)iron(III) adducts have been examined by NMR[17] and electrochemical techniques.[18] A series of binuclear hydroquinone-bridged (tetraphenylporphinato)iron(III) complexes have been characterized by magnetic, Mössbauer, and vibrational methods.[10] Non-heme iron(III) phenolate complexes have also been evaluated as relevant models for tyrosine-coordinated metalloenzymes.[19,20]

The newly prepared dimeric species described here results from the intermolecular coordination of phenolate residues in a substituted tetraarylporphyrin:

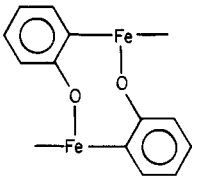

The doubly bridged phenolate structure appears to be a highly stable one. Resistance to formation of the ubiquitous μ-oxo dimer is remarkable and is unique among (tetraarylporphyrinato)iron(III) complexes lacking gross steric protection. Phenolate dimerization was discovered accidentally for a hydrolytic reaction that expectedly would have produced the μ-oxo dimer. In addition to describing the solution properties of the new intermolecular phenolate dimer, this report details the first X-ray molecular structure of a phenolate

(1) University of Iowa.
(2) University of Notre Dame.
(3) Fleischer, E. B.; Palmer, J. M.; Srivastava, T. S.; Chatterjee, A. *J. Am. Chem. Soc.* **1971**, *93*, 3162.
(4) (a) Summerville, D. A.; Cohen, I. A. *J. Am. Chem. Soc.* **1976**, *98*, 1747. (b) Scheidt, W. R.; Summerville, D. A.; Cohen, I. A. *Ibid.* **1976**, *98*, 6623.
(5) (a) Mansuy, D.; Lecomte, J.-P.; Chottard, J.-C.; Bartoli, J.-F. *Inorg. Chem.* **1981**, *20*, 3119. (b) Goedken, V. L.; Deakin, M. R.; Bottomley, L. A. *J. Chem. Soc., Chem. Commun.* **1982**, 607.
(6) (a) Phillippi, M. A.; Goff, H. M. *J. Chem. Soc., Chem. Commun.* **1980**, 455. (b) Phillippi, M. A.; Baenziger, N.; Goff, H. M. *Inorg. Chem.* **1981**, *20*, 3904.
(7) Chin, D.-H.; La Mar, G. N.; Balch, A. L. *J. Am. Chem. Soc.* **1980**, *102*, 4344.
(8) (a) Landrum, J. T.; Hatano, K.; Scheidt, W. R.; Reed, C. A. *J. Am. Chem. Soc.* **1980**, *102*, 6729. (b) Landrum, J. T.; Grimmett, D.; Haller, K. J.; Scheidt, W. R.; Reed, C. A. *Ibid.* **1981**, *103*, 2640.
(9) Fuhrhop, J.-H.; Baccouche, M.; Bünzel, M. *Angew. Chem., Int. Ed. Engl.* **1980**, *19*, 322.
(10) Kessel, S. L.; Hendrickson, D. N. *Inorg. Chem.* **1980**, *19*, 1883.
(11) (a) Dolphin, D.; Hiom, J.; Paine, J. B. *Heterocycles* **1981**, *16*, 417. (b) Collman, J. P.; Chong, A. O.; Jameson, G. B.; Oakley, R. T.; Rose, E.; Schmittou, E. R.; Ibers, J. A. *J. Am. Chem. Soc.* **1981**, *103*, 516.
(12) Reid, T. J.; Murthy, M. R. N.; Sicignano, A.; Tanaka, N.; Musick, W. D. L.; Rossman, M. G. *Proc. Natl. Acad. Sci. U.S.A.* **1981**, *78*, 4767.
(13) Bunn, H. F.; Forget, B. G.; Ranney, H. M. "Human Hemoglobins"; W. B. Saunders: Philadelphia, PA, 1977; pp 336-345.
(14) Ainscough, E. W.; Addison, A. W.; Dolphin, D.; James, B. R. *J. Am. Chem. Soc.* **1978**, *100*, 7585.
(15) Caughey, W. S.; Johnson, L. F. *J. Chem. Soc. D* **1969**, 1362.
(16) Tang, S. C.; Koch, S.; Papaefthymiou, G. C.; Foner, S.; Frankel, R. B.; Ibers, J. A.; Holm, R. H. *J. Am. Chem. Soc.* **1976**, *98*, 2414.
(17) Goff, H. M.; Shimomura, E. T.; Phillippi, M. A. *Inorg. Chem.* **1983**, *22*, 66.
(18) Phillippi, M. A.; Shimomura, E. T.; Goff, H. M. *Inorg. Chem.* **1981**, *20*, 1322.
(19) Heistand, R. H.; Lauffer, R. B.; Fikrig, E.; Que, L. *J. Am. Chem. Soc.* **1982**, *104*, 5255.
(20) Koch, S. A.; Millar, M. *J. Am. Chem. Soc.* **1982**, *104*, 5255.

0020-1669/84/1323-0315$01.50/0

(porphyrinato)iron(III) adduct. Complementary solid-state and solution results unambiguously demonstrate retention of the dimeric structure in organic solvents.

Experimental Section

Iron Porphyrin Synthesis. The asymmetric 5-(2-hydroxyphenyl)-10,15,20-tritolylporphyrin ($TTOHPH_2$) is prepared by condensation of 3 equiv of *p*-tolylaldehyde, 1 equiv of salicylaldehyde, and 4 equiv of pyrrole in a propionic acid reflux.[21] The desired porphyrin is isolated from the mixture of crystalline products by selective dissolution and by column chromatography. Warm (~50 °C) chloroform is added to the porphyrin mixture until approximately half of the solid is dissolved. The suspension is allowed to cool, and the less soluble, symmetrical tetratolylporphyrin is removed by filtration. The filtrate is subjected to chromatographic purification on both alumina and silica gel columns.[21] The previously described separation scheme was modified to the extent that methylene chloride was utilized to elute tetratolylporphyrin from the alumina column, and a 3% methanol–methylene chloride mixture was required to elute the desired porphyrin from both columns. Crystalline $TTOHPH_2$ was obtained in yields up to 6% (based on added pyrrole) by direct evaporation of the column eluent.

Iron was incorporated into the porphyrin by the standard dimethylformamide reflux method[22] utilizing anhydrous ferrous chloride (Alfa). The iron(III) derivative was precipitated from the cool dimethylformamide solution by addition of 2 volumes of aqueous 1 M HCl/0.5 M NaCl. Solid was collected on a fritted-glass funnel, air-dried, and dissolved in a minimal volume of methylene chloride. Further purification of (TTOHP)FeCl was effected on a silica gel column with elution by a 3% methanol–methylene chloride mixture. Evaporation of the major chromatographic band (with simultaneous addition of heptane) yields a microcrystalline product, which on the basis of visible[3] and proton NMR[23,24] spectra is a high-spin chloro(porphinato)iron(III) adduct (vide infra).

The dimeric phenoxide (porphinato)iron(III) complex $((TTOP)Fe)_2$ may be prepared by two alternate hydrolytic methods. Shaking a methylene chloride solution of (TTOHP)FeCl with 1.0 M aqueous NaOH solution induces a color change from brown to green (reminiscent of the green color of the (tetraphenylporphinato)iron(III) μ-oxo dimer). Passage of a methylene chloride solution of (TTOHP)FeCl through a short column of basic alumina (Fisher A-941) with elution by 5% methanol–methylene chloride also effects the same hydrolytic dimerization. Crystalline product is obtained by evaporation of the methylene chloride with addition of heptane. One molecule of heptane solvate per porphyrin unit is retained (following vacuum drying at 70 °C) as determined by proton NMR integrations. Recrystallization from hot toluene yields material that is free from solvent of crystallization as determined by the proton NMR spectrum and elemental analysis. (Anal. Calcd for $C_{94}H_{66}Fe_2N_8O_2$: C, 77.79; H, 4.58; N, 7.72. Found: C, 77.85; H, 4.65; N, 7.73.) Addition of heptane to a hot toluene solution of $((TTOP)Fe)_2$ produces well-defined crystals that on the basis of NMR integrations contain one molecule of toluene per porphyrin unit. Crystals suitable for X-ray diffraction work were obtained by slow diffusion of heptane into a toluene solution of $((TTOP)Fe)_2$.

The phenolate complex of (tetraphenylporphinato)iron(III) (TPP)FeOPh was prepared as described for natural porphyrin adducts[14] by addition of excess phenol to the iron(III) μ-oxo dimer species. To 150 mg of μ-oxo dimer in 30 mL of methylene chloride was added 3 g of phenol. Dry calcium chloride was added, and the mixture was stirred for 24 h. The solution was filtered and reduced in volume under a nitrogen stream with heptane added at intervals to crystallize the (porphinato)iron(III) product. The purple crystals were isolated by filtration, and traces of excess phenol were removed by repeated recrystallization from methylene chloride and addition of heptane. Proton NMR spectra served to characterize the complex.

Physical Measurements. Proton Fourier transform NMR spectra were recorded at 90 MHz on a JEOL FX-90Q spectrometer and at 360 MHz by Bruker WM-360 and Nicolet NT-360 instruments. Sweep widths up to 100 kHz were utilized. Solution magnetic measurements were made by the Evans method[25] at 90 MHz using toluene solutions 5 mM in iron porphyrin (concentration based on monomeric unit) and $(CH_3)_4Si$ as a reference substance. Solid-state magnetic measurements were made at ambient temperature on a Cahn 7600 Faraday susceptibility system. A 1:1 toluene/methylene chloride glass containing 1.5 mM iron porphyrin was employed for EPR measurements at 77 K on a Varian E-104A spectrometer. Cyclic voltammetric measurements were made with the Princeton Applied Research 173 potentiostat and 175 universal programmer. A standard three-electrode configuration consisted of platinum working electrode, a platinum counterelectrode, and a Ag/0.10 M $AgNO_3/CH_3CN$ reference electrode. Potentials were adjusted to the saturated calomel reference (SCE) by a factor of 0.38 V determined in our system. Visible–UV spectra of toluene solutions 10^{-4} M in (porphinato)iron complex were obtained in 0.1-cm cells on a Cary 219 spectrophotometer.

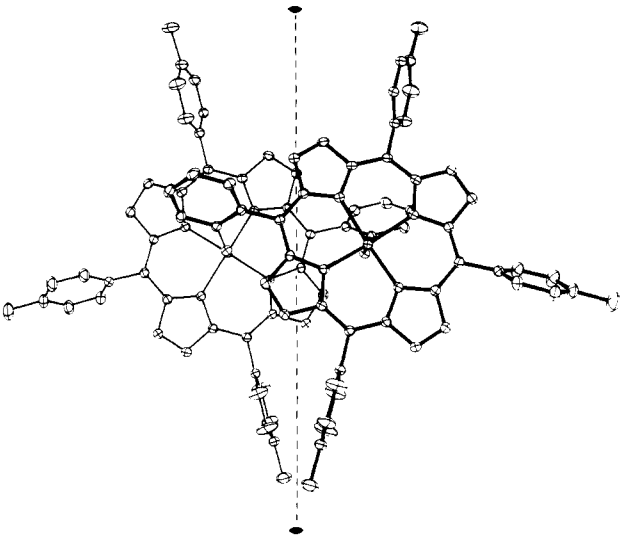

Figure 1. ORTEP plot of the $((TTOP)Fe)_2$ molecule showing overlap between the porphinato cores. The plane of the drawing is the N_4 plane of the heavy-lined core. In this figure and Figure 2, the symmetry-unique portion of the molecule is drawn with heavy bonds and the position of the crystallographically required twofold axis is displayed. All drawings are contoured at the 50% probability level.

Structure Determination. Crystals of the toluene solvate of $((TTOP)Fe)_2$ were examined on a Nicolet P$\bar{1}$ automated diffractometer. This established a two-molecule orthorhombic unit cell with possible space groups *Pmna* of *P2na* (nonstandard setting of *Pnc*2, No. 30)[26] as the possible space groups. Lattice constants, a = 16.199 (2) Å, b = 14.408 (2) Å, and c = 18.622 (3) Å, came from least-squares refinement of the setting angles of 30 reflections, each collected at $\pm 2\theta$. All measurements utilized graphite-monochromated Mo Kα radiation (λ 0.71073 Å). These constants led to a calculated density of 1.25 g/cm^3 for a cell content of $2[Fe_2O_2N_8C_{94}H_{66}\cdot 2C_7H_8]$; the measured density is 1.24 g/cm^3.

Intensity data were measured using θ–2θ scans to a maximum 2θ of 60.4°; a total of 4457 unique data were considered observed and used in the structure determination. Data were reduced as described previously.[27] With two molecules in the unit cell, the centrosymmetric space group *Pmna* would require molecular symmetry $2/m$; the noncentrosymmetric space group *P2na* requires the presence of a twofold axis of symmetry. Only the second seemed probable, and accordingly the initial structure solution was attempted in *P2na*. The structure was solved by using the direct-methods package MULTAN78.[28]

(21) Little, R. G.; Anton, J. A.; Loach, P. A.; Ibers, J. A. *J. Heterocycl. Chem.* **1975**, *12*, 343.
(22) Adler, A. D.; Longo, F. R.; Varadi, V. *Inorg. Synth.* **1976**, *16*, 213–220.
(23) La Mar, G. N.; Walker, F. A. In "The Porphyrins"; Dolphin, D., Ed.; Academic Press: New York, 1978; Vol. IV, pp 61–157.
(24) Goff, H. M. In "Iron Porphyrins—Part I"; Lever, A. B. P., Gray, H. B., Eds.; Addison-Wesley: Reading, MA, 1982; pp 237–281.
(25) Evans, D. F. *J. Chem. Soc.* **1959**, 2003.
(26) "International Tables for X-Ray Crystallography"; Kynoch Press: Birmingham, England, 1969; Vol. I, p 116.
(27) (a) Scheidt, W. R. *J. Am. Chem. Soc.* **1974**, *96*, 84. (b) A total of 6446 unique reflections were recorded in the range $3.5° \le 2\theta \le 60.4°$; of these 4457 had $F_o \ge 3\sigma(F_o)$ and were considered observed.

Table I. Fractional Coordinates[a]

Atom	X	Y	Z
Fe	0.1594	0.34367(3)	0.113166(25)
N(1)	0.26709(20)	0.42070(22)	0.11361(17)
N(2)	0.09732(19)	0.46835(22)	0.12298(17)
N(3)	0.05652(19)	0.28162(21)	0.15914(16)
N(4)	0.22658(19)	0.23379(21)	0.15321(17)
O	0.15213(19)	0.31226(16)	0.01724(12)
C(a1)	0.34557(24)	0.38377(29)	0.10739(22)
C(a2)	0.27532(25)	0.51407(27)	0.10072(20)
C(a3)	0.12817(26)	0.55647(28)	0.11162(21)
C(a4)	0.01306(25)	0.47872(26)	0.13108(22)
C(a5)	-0.02302(24)	0.31591(27)	0.15755(22)
C(a6)	0.04907(25)	0.18971(26)	0.17968(21)
C(a7)	0.19729(27)	0.14971(26)	0.17848(24)
C(a8)	0.31147(24)	0.22171(27)	0.14240(22)
C(b1)	0.40179(25)	0.4552(3)	0.08972(24)
C(b2)	0.36075(27)	0.5343(3)	0.08607(25)
C(b3)	0.06248(29)	0.62195(29)	0.11329(24)
C(b4)	-0.00832(26)	0.57550(29)	0.12494(27)
C(b5)	-0.07992(24)	0.24437(29)	0.17524(24)
C(b6)	-0.03593(28)	0.16773(26)	0.18919(24)
C(b7)	0.26489(29)	0.08602(27)	0.18542(24)
C(b8)	0.33337(26)	0.13010(29)	0.16259(25)
C(m1)	0.36570(24)	0.28899(28)	0.11838(22)
C(m2)	0.21146(26)	0.57927(28)	0.10028(21)
C(m3)	-0.04356(24)	0.40918(26)	0.14446(21)
C(m4)	0.11446(26)	0.12790(25)	0.19067(21)
C(1)	0.45319(25)	0.2608(3)	0.10454(23)
C(2)	0.51661(25)	0.28519(29)	0.15116(24)
C(3)	0.59599(27)	0.2558(4)	0.1378(3)
C(4)	0.6161(3)	0.2035(4)	0.0802(4)
C(5)	0.5542(4)	0.1792(5)	0.0345(4)
C(6)	0.4735(3)	0.2067(4)	0.0459(3)
C(7)	0.7036(4)	0.1678(5)	0.0684(5)
C(8)	0.23269(25)	0.67980(26)	0.08909(23)
C(9)	0.20198(24)	0.72885(25)	0.02998(22)
C(10)	0.22372(28)	0.82248(26)	0.02125(24)
C(11)	0.2739(3)	0.86571(28)	0.07082(28)
C(12)	0.3036(3)	0.8188(3)	0.12884(29)
C(13)	0.28276(29)	0.7270(3)	0.13921(25)
C(14)	-0.13256(24)	0.43568(28)	0.14789(23)
C(15)	-0.1829(4)	0.4259(5)	0.0910(3)
C(16)	-0.2663(4)	0.4534(6)	0.0954(5)
C(17)	-0.29853(29)	0.4920(3)	0.1550(4)
C(18)	-0.2493(4)	0.4981(5)	0.2092(3)
C(19)	-0.1670(3)	0.4710(5)	0.20728(29)
C(20)	-0.3874(4)	0.5222(5)	0.1587(5)
C(21)	0.09352(25)	0.03337(26)	0.21906(23)
C(22)	0.0600(3)	0.02186(29)	0.28563(26)
C(23)	0.0371(4)	-0.0655(3)	0.3105(3)
C(24)	0.0471(4)	-0.1422(3)	0.2686(4)
C(25)	0.0824(4)	-0.1294(3)	0.2026(4)
C(26)	0.1030(4)	-0.0440(3)	0.1769(3)
C(27)	0.0221(6)	-0.2379(4)	0.2955(5)
C(28)	0.2652(11)	0.1826(27)	0.6526(12)
C(29)	0.3140(12)	0.0835(13)	0.6437(9)
C(30)	0.3737(9)	0.0824(9)	0.5973(6)
C(31)	0.4007(8)	0.1564(10)	0.5645(5)
C(32)	0.3646(12)	0.2366(10)	0.5701(10)
C(33)	0.3029(12)	0.2378(19)	0.6147(15)
C(34)	0.4743(9)	0.1482(12)	0.5121(6)

[a] The estimated standard deviations of the least significant digits are given in parentheses.

The structure was refined by segmented full-matrix least squares. In the latter stages of refinement, hydrogen atoms were included as fixed, idealized (C–H = 0.95 Å) contributors and with anisotropic temperature factors for all heavy atoms. At convergence, R_1 was 0.049 and R_2 was 0.051.[29] Calculations for the opposite enantiomorph gave R_1 = 0.054 and R_2 = 0.057. The coordinates of the first choice are reported herein. The estimated standard deviation for an observation of unit weight is 1.50. A final difference Fourier was flat; the largest peak was 0.27 e/Å^3. Atomic coordinates are reported in Table I. Anisotropic temperature factors are tabulated in the supplementary material.

(28) Programs used in this study included local modifications of Main, Hull, Lessinger, Germain, Declerq, and Woolfson's MULTAN78, Jacobson's ALFF and ALLS, Busing and Levy's ORFFE and ORFLS, and Johnson's ORTEP2. Atomic form factors were from: Cromer, D. T.; Mann, J. B. *Acta Crystallogr., Sect. A* **1968**, *A24*, 321. Real and imaginary corrections for anomalous dispersion in the form factor of the iron atom were taken from: Cromer, D. T.; Liberman, D. *J. Chem. Phys.* **1970**, *53*, 1891. Scattering factors for hydrogen were from: Stewart, R. F.; Davidson, E. R.; Simpson, W. T. *Ibid.* **1965**, *42*, 3175.

(29) $R_1 = \sum||F_o| - |F_c||/\sum|F_o|$ and $R_2 = [\sum w(|F_o| - |F_c|)^2/\sum w(F_o)^2]^{1/2}$.

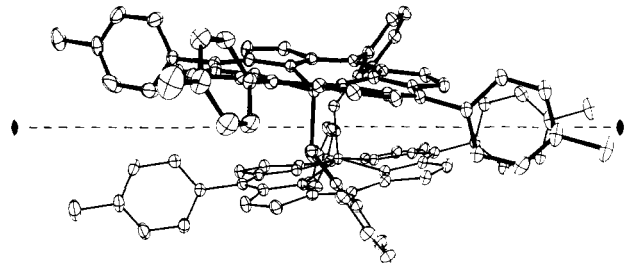

Figure 2. Second view of the ((TTOP)Fe)$_2$ molecule.

Table II. Bond Lengths (Å) in the Coordination Group and Macrocycle Skeleton[a]

Fe–O	1.847 (2)	C(b7)–C(b8)	1.347 (6)
Fe–N(1)	2.068 (3)	C(1)–C(m1)	1.497 (6)
Fe–N(2)	2.067 (3)	C(1)–C(2)	1.390 (6)
Fe–N(3)	2.076 (3)	C(1)–C(6)	1.382 (6)
Fe–N(4)	2.061 (3)	C(2)–C(3)	1.377 (6)
O–C(9)′	1.333 (5)	C(3)–C(4)	1.350 (8)
N(1)–C(a1)	1.383 (5)	C(4)–C(5)	1.361 (9)
N(1)–C(a2)	1.373 (5)	C(4)–C(7)	1.523 (7)
N(2)–C(a3)	1.381 (5)	C(5)–C(6)	1.381 (7)
N(2)–C(a4)	1.381 (5)	C(8)–C(m2)	1.503 (5)
N(3)–C(a5)	1.380 (5)	C(8)–C(9)	1.400 (6)
N(3)–C(a6)	1.383 (5)	C(8)–C(13)	1.411 (6)
N(4)–C(a7)	1.383 (5)	C(9)–C(10)	1.404 (5)
N(4)–C(a8)	1.401 (5)	C(10)–C(11)	1.378 (6)
C(a1)–C(b1)	1.413 (6)	C(11)–C(12)	1.363 (7)
C(a1)–C(m1)	1.419 (6)	C(12)–C(13)	1.378 (6)
C(a2)–C(b2)	1.440 (6)	C(14)–C(m3)	1.493 (5)
C(a2)–C(m2)	1.397 (6)	C(14)–C(15)	1.344 (7)
C(a3)–C(b3)	1.422 (6)	C(14)–C(19)	1.339 (7)
C(a3)–C(m2)	1.405 (6)	C(15)–C(16)	1.411 (8)
C(a4)–C(b4)	1.441 (6)	C(16)–C(17)	1.346 (9)
C(a4)–C(m3)	1.381 (6)	C(17)–C(18)	1.290 (8)
C(a5)–C(b5)	1.421 (5)	C(17)–C(20)	1.506 (7)
C(a5)–C(m3)	1.406 (5)	C(18)–C(19)	1.389 (7)
C(a6)–C(b6)	1.424 (6)	C(21)–C(m4)	1.500 (5)
C(a6)–C(m4)	1.399 (6)	C(21)–C(22)	1.364 (6)
C(a7)–C(b7)	1.434 (6)	C(21)–C(26)	1.372 (6)
C(a7)–C(m4)	1.397 (5)	C(22)–C(23)	1.391 (6)
C(a8)–C(b8)	1.418 (6)	C(23)–C(24)	1.363 (7)
C(a8)–C(m1)	1.383 (6)	C(24)–C(25)	1.367 (8)
C(b1)–C(b2)	1.321 (6)	C(24)–C(27)	1.521 (7)
C(b3)–C(b4)	1.345 (6)	C(25)–C(26)	1.362 (7)
C(b5)–C(b6)	1.340 (6)		

[a] The numbers in parentheses are the estimated standard deviations. Primed and unprimed symbols denote a pair of atoms related by the twofold axis.

Results and Discussion

Structure of ((TTOP)Fe)$_2$. The dimeric molecule is shown in two different orientations in Figures 1 and 2, which display aspects of the intermolecular arrangement along with the relative position of the crystallographically required twofold axis of symmetry. In each drawing, the crystallographically unique portion of the molecule is displayed with heavy bonds. As is clear from Figure 1, there is a modest overlap between the two porphinato cores in the molecule. The closest approach is a 3.34-Å contact between β-pyrrole carbon atoms. (These occur at the bottom of Figure 1 and at the right in Figure 2.) However, the average perpendicular separation between the atoms of one core and the mean plane of the other core is 4.09 Å as a result of the 13.5° dihedral angle between the two cores (Figure 2). There are thus, at most, very modest π–π interactions between the two cores in the molecule.

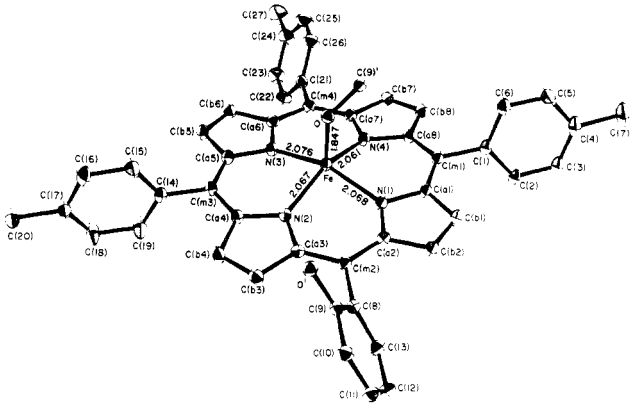

Figure 3. Symmetry-unique portion of the $((TTOP)Fe)_2$ molecule displaying the atom labels and the bond distances in the coordination group.

Table III. Bond Angles (deg) in the Coordination Group and Macrocycle Skeleton[a]

OFeN(1)	100.91 (12)	C(b4)C(a4)C(m3)	123.8 (4)
OFeN(2)	105.51 (12)	N(3)C(a5)C(b5)	109.9 (3)
OFeN(3)	104.02 (12)	N(3)C(a5)C(m3)	124.5 (3)
OFeN(4)	101.28 (12)	C(b5)C(a5)C(m3)	125.4 (4)
N(1)FeN(2)	86.77 (13)	N(3)C(a6)C(b6)	109.4 (3)
N(2)FeN(3)	86.97 (12)	N(3)C(a6)C(m4)	125.7 (4)
N(3)FeN(4)	86.78 (12)	C(b6)C(a6)C(m4)	124.9 (4)
N(4)FeN(1)	88.02 (12)	N(4)C(a7)C(b7)	109.2 (4)
N(1)FeN(3)	155.07 (13)	N(4)C(a7)C(m4)	125.6 (4)
N(2)FeN(4)	153.21 (13)	C(b7)C(a7)C(m4)	125.1 (4)
FeOC(9)'	135.11 (25)	N(4)C(a8)C(b8)	108.9 (4)
FeN(1)C(a1)	124.66 (26)	N(4)C(a8)C(m1)	125.7 (4)
FeN(1)C(a2)	127.39 (27)	C(b8)C(a8)C(m1)	125.4 (4)
C(a1)N(1)C(a2)	105.8 (3)	C(a1)C(b1)C(b2)	108.4 (4)
FeN(2)C(a3)	127.56 (26)	C(a2)C(b2)C(b1)	107.4 (4)
FeN(2)C(a4)	125.76 (27)	C(a3)C(b3)C(b4)	108.1 (4)
C(a3)N(2)C(a4)	105.9 (3)	C(a4)C(b4)C(b3)	106.8 (4)
FeN(3)C(a5)	125.90 (24)	C(a5)C(b5)C(b6)	107.3 (4)
FeN(3)C(a6)	126.59 (26)	C(a6)C(b6)C(b5)	107.9 (4)
C(a5)N(3)C(a6)	105.5 (3)	C(a7)C(b7)C(b8)	107.4 (3)
FeN(4)C(a7)	127.93 (26)	C(a8)C(b8)C(b7)	108.4 (4)
FeN(4)C(a8)	124.18 (27)	C(a1)C(m1)C(a8)	125.1 (4)
C(a7)N(4)C(a8)	106.1 (3)	C(a1)C(m1)C(1)	117.0 (3)
N(1)C(a1)C(b1)	109.4 (3)	C(a8)C(m1)C(1)	117.8 (4)
N(1)C(a1)C(m1)	124.7 (3)	C(a2)C(m2)C(a3)	123.6 (4)
C(b1)C(a1)C(m1)	125.9 (4)	C(a2)C(m2)C(8)	118.6 (4)
N(1)C(a2)C(b2)	109.0 (4)	C(a3)C(m2)C(8)	117.8 (4)
N(1)C(a2)C(m2)	126.0 (4)	C(a4)C(m3)C(a5)	124.6 (4)
C(b2)C(a2)C(m2)	125.0 (4)	C(a4)C(m3)C(14)	117.6 (4)
N(2)C(a3)C(b3)	109.6 (4)	C(a5)C(m3)C(14)	117.8 (4)
N(2)C(a3)C(m2)	125.8 (4)	C(a6)C(m4)C(a7)	124.1 (4)
C(b3)C(a3)C(m2)	124.5 (4)	C(a6)C(m4)C(21)	117.3 (4)
N(2)C(a4)C(b4)	109.5 (4)	C(a7)C(m4)C(21)	118.6 (4)
N(2)C(a4)C(m3)	126.7 (4)		

[a] Figures in parentheses are the estimated standard deviations in the least significant figure. Primed and unprimed symbols denote a pair of atoms related by the twofold axis.

Figure 3 presents the labeling scheme for the crystallographically unique atoms. The diagram also displays bond distances in the coordination group. Individual bond distances and bond angles are listed in Tables II and III, respectively. Primed and unprimed symbols, e.g., C(i) and C(i)', denote a pair of atoms related by the twofold axis of symmetry. By using C(a) and C(b) to denote the α- and β-carbon atoms of a pyrrole ring, C(m) for the methine carbon atoms, and C(p) for aryl carbon atoms, average values for the chemically distinct bond parameters can be noted. The values for the bond distances in the core are N–C(a) = 1.383 (8) Å, C(a)–C(b) = 1.427 (10) Å, C(b)–C(b) = 1.338 (12) Å, C(a)–C(m) = 1.398 (12) Å, and C(m)–C(p) = 1.498 (4) Å. The number in parentheses in these and subsequent averaged values is the estimated standard deviation for the average. Averaged values

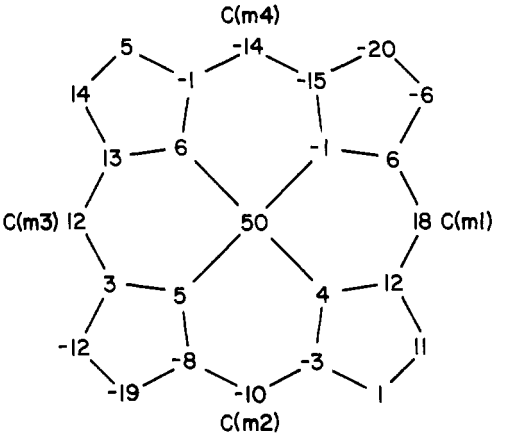

Figure 4. Formal diagram of the porphinato core in $((TTOP)Fe)_2$ displaying the perpendicular displacements of the atoms, in units of 0.01 Å, from the mean plane of the 24-atom core. The four methine carbon atoms are labeled. Positive displacements are toward the center of the $((TTOP)Fe)_2$ molecule.

for bond angles are C(a)NC(a) = 105.8 (3)°, NC(a)C(m) = 125.6 (7)°, NC(a)C(b) = 109.4 (3)°, C(a)C(b)C(b) = 107.7 (6)°, C(a)C(m)C(a) = 124.4 (6)°, and C(m)C(a)C(b) = 125.0 (6)°. Averaged values for the C–C distance in the peripheral aryl groups are 1.371 (27) Å, and C(p)–CH_3 = 1.517 (9) Å.

The average Fe–N(p) distance of 2.068 (6) Å, the 0.46-Å displacement of the iron atom from the mean plane of the four nitrogen atoms, and the 0.50-Å displacement from the mean plane of the 24-atom core are in accord with expectation values from other five-coordinate high-spin (porphinato)iron(III) species.[30] It is possible that the intramolecular axial ligand constraints have a small effect on the (nonequal) Fe–N(p) bond distances; the Fe–O vector is tipped from the heme normal by ~3.5° (away from N(1) and N(3)). However, there is no apparent effect on the length of the Fe–O (phenolate) bond distance, which is 1.847 (2) Å. This value is quite comparable to the 1.842 (4) Å Fe–O bond distance found for the methoxyiron(III) derivative of mesoporphyrin IX dimethyl ester[31] and two five-coordinate iron(III) phenolate complexes of salen and saloph[32] (1.861 (2) and 1.828 (4) Å, respectively). The distance is also close to the average Fe–O distances of 1.847 (3) and 1.866 (6) Å found for two tetrahedral iron(III) phenolate complexes.[20] Fe–O distances in the FeO_6 cores of $[Fe^{III}(catecholate)_3]^{3-}$ complexes[33] are significantly larger at 2.02 Å. It is to be noted that the pattern of a short axial bond, relative to typical high-spin values for otherwise similar six-coordinate complexes is common in five-coordinate (porphinato)iron(III) complexes. The FeOC(9)' angle of 135.11 (25)° is well within the range of values for phenolate complexes. The FeOC(9)' plane forms dihedral angles of 54.3° with the N(1)FeO coordinate plane and 35.8° with the N(4)FeO plane.

The dihedral angle between the phenolate plane and its covalently attached porphinato core is 61.8°. Although this angle is at the low end of the range of values observed in tetraphenylporphinato species, it is still within normal values. The dihedral angles between the three *p*-tolyl groups and the

(30) Scheidt, W. R.; Reed, C. A. *Chem. Rev.* **1981**, *81*, 543.
(31) Hoard, J. L.; Hamor, M. J.; Hamor, T. J.; Caughey, W. S. *J. Am. Chem. Soc.* **1965**, *87*, 2312.
(32) Heistand, R. H.; Roe, A. L.; Que, L. *Inorg. Chem.* **1982**, *21*, 676. salen is the abbreviation for the bis[*N*,*N*'-ethylenebis(salicylideneaminato)] anion and saloph for the *N*,*N*'-(1,2-phenylene)bis(salicylideneaminato) anion.
(33) (a) Anderson, B. F.; Buckingham, D. A.; Robertson, G. B.; Webb, J.; Murray, K. S.; Clark, P. E. *Nature (London)* **1976**, *262*, 722. (b) Raymond, K. N.; Isied, S. S.; Brown, L. D.; Fronczek, F. R.; Nibert, J. H. *J. Am. Chem. Soc.* **1976**, *98*, 1767.

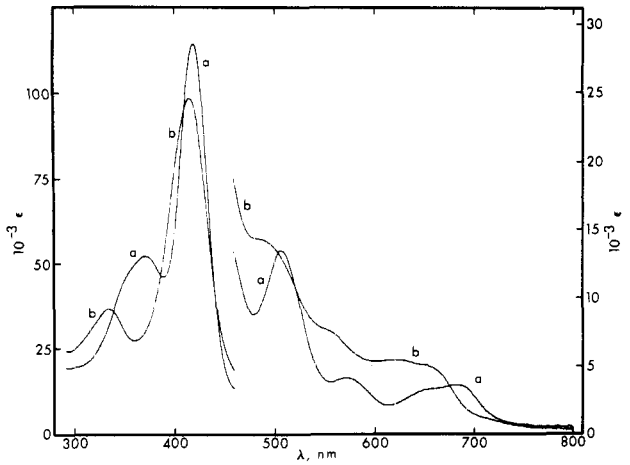

Figure 5. Electronic spectra of (porphinato)iron(III) complexes 1.36 × 10^{-4} M in toluene solution for (a) (TTOHP)FeCl and (b) ((TTOP)Fe)$_2$. Concentration and molar absorptivity values are based on the monomeric unit.

core are 71.3, 63.2, and 85.9°. Figure 4 displays the perpendicular displacement of the atoms of the core, in units of 0.01 Å, from the best plane of the 24-atom core. As can be seen from the figure, the porphinato core exhibits a modest quasi-S_4 ruffling that is well within the limits of porphinato core conformations observed.[34]

The separation between the two iron atoms in the molecule is 6.169 (1) Å. Intermolecular Fe···Fe separations range from 9.57 Å upward. There are no unreasonable inter- or intramolecular contacts. The shortest intermolecular contacts involve aryl carbon atoms to adjacent porphinato core atoms and are 3.49 Å. The toluene solvate molecules are also well separated in the lattice with only one intermolecular contact less than 3.75 Å (C(32)···C(b4) = 3.55 Å).

Electronic Spectra. Figure 5 reveals that the electronic spectrum of (TTOHP)FeCl is much like that expected for a chloro(tetraphenylporphinato)iron(III) complex.[3] Absorption bands at 370, 420 (Soret), 506, 572, 652, and 684 nm are reminiscent of values for (TPP)FeCl of 380, 417 (Soret), 511, 577, 658, and 690 nm.[3] Small differences in band positions are most likely due to the electron-releasing character of tolyl and 2-hydroxyphenyl groups in (TTOHP)FeCl. Under basic conditions the 2-hydroxyphenyl group is deprotonated, and the spectrum of ((TTOP)Fe)$_2$ in Figure 5 appears to be that of a phenoxide (porphinato)iron(III) complex. Absorption bands at 334, 416 (Soret), 488, 556, 620, and 656 nm for ((TTOP)Fe)$_2$ parallel those at 330, 412 (Soret), 490, 555, 610, and 647 nm for (TPP)FeOPh. The phenoxide ligand thus induces significant spectral changes, but the electronic spectrum retains the features of a five-coordinate high-spin iron(III) complex. Analogous differences are seen for the halide and phenoxide complexes of (protoporphinato)iron(III).[14] The electronic spectrum of ((TTOP)Fe)$_2$ also resembles that for the dimeric hydroquinone complex of (tetraphenylporphinato)iron(III).[10]

Magnetic Properties. Ambient-temperature solid-state and solution measurements support a high-spin iron(III) assignment for ((TTOP)Fe)$_2$. A magnetic moment value of 5.91 ± 0.05 μ_B per iron atom was obtained at 28 °C in the solid state, and an equivalent value of 6.0 ± 0.2 μ_B was measured for a toluene solution of the same compound. The phenoxide bridges of ((TTOP)Fe)$_2$ thus do not promote significant superexchange between the iron centers. The absolute value of

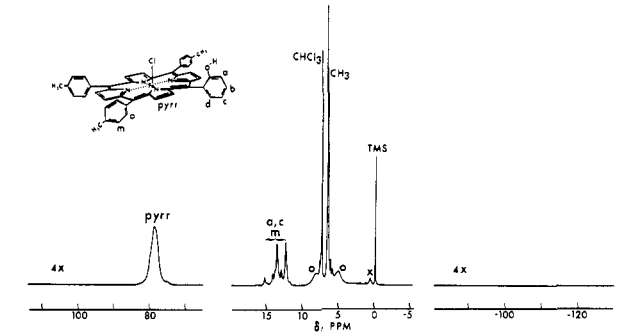

Figure 6. Proton NMR spectrum of (TTOHP)FeCl (concentration 0.01 M, $CDCl_3$ solvent, $(CH_3)_4Si$ reference, 25 °C, spectrometer frequency 360 MHz). The × signal in the 1.0 ppm region is due to a $CDCl_3$ trace water impurity and is broadened by exchange with the phenol OH.

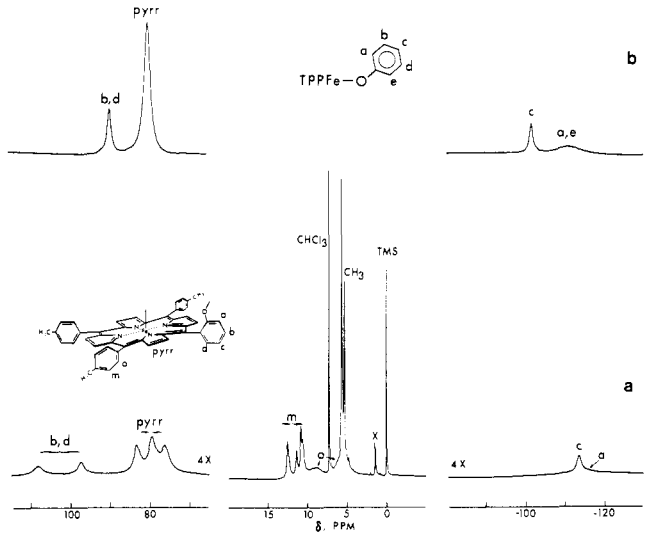

Figure 7. Proton NMR spectra of phenolate (porphinato)iron(III) complexes (concentration 0.01 M on a monomeric basis, $CDCl_3$ solvent, $(CH_3)_4Si$ reference, 25 °C, spectrometer frequency 360 MHz): (a) ((TTOP)Fe)$_2$; (b) (TPP)FeOPh, far-upfield and -downfield regions only. The × signal in the 1.0 ppm region is due to a $CDCl_3$ trace water impurity.

J must be less than 5 cm^{-1}. In this context it should be noted that direct bridging by deprotonated hydroquinone ligands elicits weak antiferromagnetic exchange interactions with J values ranging from −3.6 to −15.5 cm^{-1}.[10]

Although coupling between metal atoms in ((TTOP)Fe)$_2$ is not large, proximity of two paramagentic centers (6.2 Å between iron atoms) induces spin–spin relaxation such that no EPR spectrum is detectable for ((TTOP)Fe)$_2$ in a 1:1 toluene/methylene chloride glass at 77 K. Under identical solution and instrument conditions, strong g = 5.6 and 2.0 signals were observed for (TPP)FeOPh.

Nuclear Magnetic Resonance Measurements. The proton NMR spectrum of (TTOHP)FeCl in Figure 6 is diagnostic for that of a five-coordinate high-spin (tetraphenylporphinato)iron(III) complex.[23,24] Resolution of the four sets of pyrrole proton signals near 80 ppm is not apparent, although the line shape is suggestive of overlapping peaks. Splitting of *m*-tolyl signals in the 12–15 ppm region is induced by the out-of-plane iron atom that leads to inequivalence of protons on slowly rotating, orthogonal groups. Small signals in the 12–15 ppm region are presumably from the 2-hydroxyphenyl group, which can have two possible orientations with respect to the iron–chloride linkage. Broad *o*-tolyl signals are located at 5 and 8 ppm. Absence of signals in the far-upfield region should be noted for Figure 6.

(34) (a) Hoard, J. L. In "Porphyrins and Metalloporphyrins"; Smith, K. M., Ed.; Elsevier: Amsterdam, 1975; pp 317–380. (b) Scheidt, W. R. In "The Porphyrins"; Dolphin, D., Ed.; Academic Press: New York, 1978; Vol. III, pp 463–511.

A high-field proton NMR spectrum of $((TTOP)Fe)_2$ in Figure 7a is most revealing in electronic and molecular structural terms. The new twofold symmetry of the macrocycle is apparent in the magnified splitting of pyrrole proton signals at 83.2, 79.4, and 76.1 ppm. Signals for *m*-tolyl protons in the 11–13 ppm region are shifted slightly upfield as compared with those for the chloro complex (Figure 6). The *m*-tolyl region is also simplified and consists of two doublets (splitting from the out-of-plane iron atom) with a 2:1 intensity pattern expected for a molecule with twofold symmetry. Tolyl methyl signals are likewise split into a 2:1 intensity pattern. This pattern of porphyrin signals is overall consistent with a high-spin iron(III) configuration. An average pyrrole proton chemical shift value of 80 ppm indicates negligible antiferromagnetic coupling as was also demonstrated by magnetic measurements. No μ-oxo dimeric product is detected as this species would exhibit a pyrrole proton signal in the 13 ppm region and tolyl proton resonances near 7.6 ppm.

In addition to the far-downfield pyrrole proton signals in Figure 7a, resonances are noted at 108.3, 97.4, −113.4, and −115 (very broad) ppm. These signals are from the 2-hydroxyphenyl group, which is deprotonated and coordinated in an intermolecular manner with a second iron center. Assignments of far-downfield and -upfield peaks are made by comparison with the spectrum of (TPP)FeOPh in Figure 7b and with spectra of other substituted and appended phenolate (porphinato)iron(III) complexes.[35] Assignments in Figure 7 are consistent with those recently made for phenolate complexes of iron(III) salen.[19] The far-downfield assignment for phenolate bound to (protoporphinato)iron(III) is also in agreement with our result, but the relatively sharp far-upfield signal was originally assigned to 2,6-phenolate protons rather than to the 4-proton.[15]

Reversible interconversion of dimeric $((TTOP)Fe)_2$ to monomeric (TTOHP)FeCl is demonstrated by experiments in which a solution of HCl in methanol was titrated into an NMR tube. The proton NMR spectrum shown in Figure 7a was converted to that of Figure 6 upon addition of 2 equiv of HCl (per dimeric unit). Addition of a small volume of aqueous NaOH solution followed by vigorous shaking of the NMR tube served to regenerate dimeric $((TTOP)Fe)_2$.

Chemical reduction of $((TTOP)Fe)_2$ is possible, and the iron(II) product has been characterized by proton NMR spectroscopy. Reduction is effected by sequential addition of deoxygenated toluene-d_8 and 0.02 mL of D_2O to a septum-sealed, nitrogen-flushed NMR tube containing solid $((TTOP)Fe)_2$ and sodium dithionite. The tube is shaken vigorously, and the aqueous layer is allowed to settle over a period of hours. Proton NMR examination of the sample prior to complete reduction reveals signals only for the parent iron(III) $((TTOP)Fe)_2$ species and the iron(II) product. On the basis of a diagnostic hyperfine NMR shift pattern,[23,24,36] the reduced product is identified as an intermediate-spin (porphinato)iron(II). Multiplets in the 20, 12, and 4 ppm regions match signals in $(TPP)Fe^{II}$ for *o*-tolyl, *m*-tolyl, and pyrrole protons. Respective signals for the 2-hydroxyphenyl group add some complexity to the 20 and 12 ppm resonances. Previously characterized $S = 1$ (porphinato)iron(II) derivatives are four-coordinate, and addition of a weak axial ligand is presumably associated with conversion to the $S = 2$ state. Thus, reduction of $((TTOP)Fe)_2$ is associated with cleavage of the iron–phenoxide linkage to form a four-coordinate monomeric ferrous product. Further support for this formulation is based on the absence of upfield signals for a coordinated 2-hydroxyphenyl residue. Intermediate-spin iron(II) exhibits high magnetic anisotropy and would induce large upfield (of $(CH_3)_4Si$) dipolar proton chemical shifts in any residue placed in an axial position.

In contrast to other (tetraphenylporphinato)iron(III) adducts, which almost universally undergo base hydrolysis to form the μ-oxo dimeric species, the 2-hydroxyphenyl derivative exhibits a remarkable propensity to form the bridged phenoxide dimer. Autoxidation of ferrous porphyrins is also generally associated with μ-oxo dimer formation. However, air oxidation of $(TTOP)Fe^{II}$ in "wet" toluene solution yields $((TTOP)Fe)_2$ as the only major (final) product as discerned by proton NMR and electronic spectral measurements.

Electrochemical Measurements. The basic phenoxide residue provides a much stronger ligand for iron(III) than for iron(II), and hence reduction potentials for phenoxide (porphinato)iron(III) complexes are among the most cathodic of high-spin complexes.[14,17] Cyclic voltammetric scans reveal a series of complex redox processes for $((TTOP)Fe)_2$. Reversible reductions occur at −0.70 and −0.87 V and are reasonably assigned to sequential Fe(III) → Fe(II) processes. The −0.70 V value is in logical agreement with the first reduction potential of −0.66 V for (TPP)FeOPh given the electron-releasing groups on $((TTOP)Fe)_2$. The two reduction waves of interest are cleanly reversible at scan rates as low as 20 mV/s, indicating that dissociation of two bridged iron(II) centers (as discerned by NMR measurements) is relatively slow on the cyclic voltammetric time scale.

Overlapping oxidation waves are observed for $((TTOP)Fe)_2$ with reversible or quasi-reversible features at +0.93, +1.14, +1.43, and +1.50 V. Oxidation may take place at the metal center, the porphyrin π-system, or the coordinated phenoxide residue. The first oxidation wave in simple five-coordinate, high-spin (tetraarylporphinato)iron(III) adducts corresponds to electron abstraction from the porphyrin ring. This potential is approximately 1.1 V for a series of (TPP)FeX complexes.[18] In general, only one additional reversible wave is observed near +1.35 V for monomeric (TPP)FeX species.[37] The oxidation profile of $((TTOP)Fe)_2$ is thus clearly perturbed with respect to that for monomeric complexes. The cathodic shift of the first oxidation potential to 0.93 V cannot be rationalized by porphyrin ring substituents, as the value for $(TPP(p\text{-}OCH_3))FeCl$ is 1.02 V.[38] The unusual 0.93-V wave may reflect metal-centered or phenoxide oxidation rather than porphyrin-ring oxidation.

Conclusions. Dimerization through phenoxide units rather than a μ-oxo linkage is preferred as a consequence of the high affinity of iron(III) for phenoxide and the fact that two bridges are formed per dimeric unit. Favorable stability of the double bridge and steric constraints apparently preclude formation of polymeric units. Porphyrin-core structural parameters for $((TTOP)Fe)_2$ are rather unremarkable as compared with other five-coordinate high-spin ferric complexes. The iron–oxygen distance of 1.847 Å is comparable to the ligand–metal distance in related molecules. The iron–oxygen bond is only 3° from the vertical, thereby indicating no large degree of "strain" in forming the dimeric structure. Lack of significant spin–spin exchange in $((TTOP)Fe)_2$ is reasonable considering the indirect orbital overlap possible for this dimer, as compared with the more direct (yet relatively inefficient) overlap possible for quinone[10] and sulfate[6] bridges.

The multiple redox steps observed for $((TTOP)Fe)_2$ imply that the dimer can potentially serve as a binuclear multielectron oxidative catalyst or, in the reduced mononuclear form, as a mediator for the reduction and activation of dioxygen species. A particularly attractive feature of $((TTOP)Fe)_2$

(35) Shimomura, E. T.; Goff, H. M., manuscript in preparation.
(36) Goff, H.; La Mar, G. N.; Reed, C. A. *J. Am. Chem. Soc.* **1977**, *99*, 3641.
(37) Kadish, K. M. In "Iron Porphyrins—Part II"; Lever, A. B. P., Gray, H. B., Eds.; Addison-Wesley: Reading, MA, 1983; pp 161–249.
(38) Phillippi, M. A.; Goff, H. M. *J. Am. Chem. Soc.* **1982**, *104*, 6026.

relevant to the problem of dioxygen reduction is the absence of μ-oxo formation. Evaluation of $((TTOP)Fe)_2$ as a useful electrocatalyst is in progress.

Acknowledgment. We are grateful to Arden Boersma and Gregory Godziela for repetition of electrochemical measurements and synthetic procedures. Preliminary high-field NMR measurements were made at the Colorado State University Regional NMR Center, funded by National Science Foundation Grant No. CHE 78-18581. The Bruker WM-360 NMR spectrometer at the University of Iowa was purchased in part by NSF Grant No. CHE 82-01836. Support from the National Science Foundation, Grants CHE 79-10305 and CHE 82-09308 (H.M.G.), and the National Institutes of Health, Grants GM-28831 (H.M.G.) and HL-15627 (W.R.S.), is gratefully acknowledged.

Registry No. $((TTOP)Fe)_2$, 88200-64-0; $((TTOP)Fe)_2 \cdot 2C_7H_8$, 88200-65-1; (TTOHP)FeCl, 88200-66-2; (TPP)FeOPh, 76282-28-5.

Supplementary Material Available: Anisotropic temperature factors (Table IV), fixed hydrogen atom positions and isotropic temperature factors (Table V), and a listing of observed and calculated structure factor amplitudes (×10) (18 pages). Ordering information is given on any current masthead page.

Contribution from the Department of Chemistry, University of Iowa, Iowa City, Iowa 52242

Carbon-13 and Deuterium NMR Spectroscopy of High-Spin Manganese(III) Porphyrin Halide and Pyridine Complexes

HAROLD M. GOFF* and ANDREW P. HANSEN

Received September 8, 1982

Carbon-13 NMR spectroscopic measurements have been performed for high-spin manganese(III) porphyrins to evaluate effects of axial ligand binding and to correlate isotropic shift patterns with d-orbital occupation. A qualitative description of unpaired spin delocalization mechanisms is offered. No particular ordering of resonances is apparent for F^-, Cl^-, and I^- adducts, but absolute shift values for the F^- complex are larger and approach those for the stronger field 4-methylpyridine ligand. Resonances for α-pyrrole carbon atoms are downfield and cover a range from 383 to 492 ppm. Corresponding β-pyrrole carbon signals are upfield in the region from −72 to −166 ppm. The meso carbon signal exhibits a small upfield shift, which increases in magnitude with 4-methylpyridine displacement of the halide ligand. Previously elucidated carbon-13 shift correlations are consistent with predominant unpaired π-spin density at β-pyrrole and meso carbon sites of manganese(III) porphyrins. Negative π-spin density at the meso carbon atom is to be contrasted with earlier Hückel calculations that predict large positive spin density at this position. Deuterium NMR spectroscopy revealed large downfield shifts for α- and β-deuterium atoms of coordinated pyridine-d_5. Corresponding carbon-13 signals are also far downfield. These observations are readily explained by transmission of σ-spin density from the singly occupied d_{z^2} orbital to the axial pyridine ligand.

Introduction

Nuclear magnetic resonance spectroscopy of paramagnetic complexes potentially can yield information about magnetic anisotropy, d-orbital occupation, unpaired spin delocalization mechanisms, and perturbations of electronic structure. Paramagnetic metalloporphyrins have been the subject of numerous proton NMR studies, and correlatons between shift patterns and d-orbital occupation are well-established.[1,2] Such results have important biological implications and applications. In physical–inorganic terms, metalloporphyrin complexes also provide a rigid, well-defined ligand system for developing a general understanding of carbon-13 paramagnetic shifts. The information content of carbon-13 spectra is especially great, but separation of the various shift contributions is correspondingly more difficult than is the case for proton spectra. The challenge to delineate carbon-13 shift mechanisms has inspired systematic examination of high-spin iron(III),[3-10] low-spin iron(III),[3,11-15] admixed-spin iron(III),[16] μ-oxo dimeric iron(III),[3,4] high-spin iron(II),[17] and low-spin cobalt(II)[18] porphyrin complexes.

The work reported here focuses on using high-spin manganese(III) porphyrin complexes to test our expectations relating electronic structure with carbon-13 NMR shift patterns. Effects of changing the axial ligand are investigated. A qualitative description of unpaired spin delocalization mechanisms is offered on the basis of comparative carbon-13, proton, and deuterium NMR shift patterns. Results complement earlier proton NMR interpretations and theoretical calculations and at the empirical level could be used to distinguish the +3 oxidation state of manganese porphyrins.

Experimental Section

Manganese(III) porphyrin complexes were prepared by the standard dimethylformamide reflux method.[19] A solution of the crude product in methylene chloride was shaken with 1 M aqueous sodium hydroxide, and the organic layer was subjected to column chromatographic purification on alumina. The resulting "hydroxo" manganese(III) porphyrin was converted to the halide complex by stirring a methylene chloride solution with the appropriate 1 M aqueous acid. Crystalline product was formed by addition of heptane to a concentrated methylene chloride solution of the manganese(III) porphyrin. Products were routinely vacuum-dried at 100 °C. Proton NMR spectra,[20,21] UV–vis spectra,[22] and thin-layer chromatography confirmed the identity and

(1) La Mar, G. N.; Walker, F. A. In "The Porphyrins"; Dolphin, D., Ed.; Academic Press: New York, 1979, Vol. IV, pp 61-157.
(2) Goff, H. M. In "Iron Porphyrins—Part I"; Lever, A. B. P., Gray, H. B., Eds.; Addison-Wesley: Reading, MA, 1982; pp 237-281.
(3) Goff, H. M.; Morgan, L. O. *Bioinorg. Chem.* **1978**, *9*, 61.
(4) Goff, H. *Biochim. Biophys. Acta* **1978** *542*, 348.
(5) Mispelter, J.; Momenteau, M.; Lhoste, J.-M. *J. Chem. Soc., Chem. Commun.* **1979**, 808.
(6) Phillippi, M. A.; Goff, H. M. *J. Chem. Soc., Chem. Commun.* **1980**, 455.
(7) Mispelter, J.; Momenteau, M.; Lhoste, J.-M. *J. Chem. Soc., Dalton Trans.* **1981**, 1729.
(8) Phillippi, M. A.; Baenziger, N.; Goff, H. M. *Inorg. Chem.* **1981**, *20*, 3904.
(9) Behere, D. V.; Mitra, S. *Proc. Indian Acad. Sci. Sect. X* **1982**, *91X*, 145.
(10) Goff, H. M.; Shimomura, E. T.; Phillippi, M. A. *Inorg. Chem.* **1983**, *22*, 66.
(11) Wüthrich, K.; Baumann, R. *Helv. Chim. Acta* **1973**, *56*, 585.
(12) Wüthrich, K.; Baumann, R *Helv. Chim. Acta* **1974**, *57*, 336.
(13) Goff, H. *J. Chem. Soc., Chem. Commun.* **1978**, 777.
(14) La Mar, G. N.; Viscio, D. B.; Smith, K. M.; Caughey, W. S.; Smith, M. L. *J. Am. Chem. Soc.* **1978**, *100*, 8085.
(15) Goff, H. M. *J. Am. Chem. Soc.* **1981**, *103*, 3714.
(16) Boersma, A. D.; Goff, H. M. *Inorg. Chem.* **1982**, *21*, 581.
(17) Shirazi, A.; Leum, E.; Goff, H. M. *Inorg. Chem.* **1983**, *22*, 360.
(18) Shirazi, A.; Goff, H. M. *Inorg. Chem.* **1982**, *21*, 3420.
(19) Adler, A. D.; Longo, F. R.; Varadi, V. *Inorg. Synth.* **1976**, *16*, 213.
(20) La Mar, G. N.; Walker, F. A. *J. Am. Chem. Soc.* **1973**, *95*, 6950.
(21) La Mar, G. N.; Walker, F. A. *J. Am. Chem. Soc.* **1975**, *97*, 5103.

0020-1669/84/1323-0321$01.50/0